

Interaction of EMIC Waves with Thermal Plasma and Radiation Belt Particles

Richard M. Thorne¹, Richard B. Horne², Vania K. Jordanova³, Jacob Bortnik¹, and Sarah Glauert²

¹ *Department of Atmospheric and Oceanic Sciences, University of California, Los Angeles, California.*

² *British Antarctic Survey, Natural Environment Research Council, Cambridge, UK.*

³ *Space Science Center, University of New Hampshire, Durham, New Hampshire.*

Electromagnetic ion cyclotron waves are excited during the enhanced convective injection of plasmashet ions into the inner magnetosphere. Waves grow rapidly near the magnetic equatorial plane reaching amplitudes up to 10 nT. Such intense waves induce scattering of cyclotron resonant ions at a rate comparable to the strong diffusion limit, causing rapid ion precipitation into the atmosphere in localized regions where the waves are present. The waves also resonate with relativistic electrons at energies typically above 0.5 MeV. Such scattering, which could provide a major loss process for relativistic outer zone electrons during the main phase of a magnetic storm, is confined to high-density regions just inside the plasmopause or within dayside drainage plumes. As EMIC waves propagate to higher latitude, their wave normal angle becomes highly oblique. This allows Landau resonant interaction with thermal electrons, which can heat the electron population in the outer plasmasphere to several eV, contributing to the heat flux that drives Stable Auroral Red (SAR) arcs. During the propagation to higher latitude, EMIC waves can also experience cyclotron resonant damping by heavy thermal ions, leading to ion conic distributions, which are observed near the equator.

1. INTRODUCTION

1.1. Radiation Belt Dynamics.

The Earth's radiation belts are comprised of energetic ions and electrons trapped in orbits within the basically dipolar terrestrial magnetic field. Under adiabatic conditions, the particle orbits can be treated under the guiding center approximation as a combination of gyro motion around the field, bounce motion between magnetic mirror points, and drift motion due to gradients in the field and other forces [Roederer, 1970]. Under adiabatic theory, those particles with magnetic mirror points within the dense atmosphere (i.e., those with pitch-angles inside the loss cone) are removed within a bounce period, while those mirroring at high altitude remain trapped for long periods of time. The radiation belts, however, respond dramatically to solar disturbances. Particles are both accelerated to high energy, and scattered in pitch-angle, leading to ultimate loss to the atmosphere. Such non-adiabatic behavior can be caused by resonant interactions with various plasma

waves. Here we will consider the significance of scattering caused by electromagnetic ion cyclotron (EMIC) waves.

1.2. Properties of Magnetospheric EMIC Waves.

EMIC waves are an important constituent of the magnetospheric plasma. They strongly affect the dynamics of resonant radiation belt particles, leading to either non-adiabatic heating or precipitation loss. The properties of EMIC waves have been studied from both ground-based observation and satellites for several decades, and a comprehensive review of such observations is presented in Chapter 14 of this monograph [Fraser, 2006]. EMIC waves are excited in the magnetosphere by cyclotron resonant instability (section 2) with anisotropic medium-energy ring current ions. Typical measured wave amplitudes lie in the range 0.1-10 nT, with the most intense waves present during the main phase of magnetic storms [e.g., *Braysy et al.*, 1998; *Erlandson and Ukhorskiy*, 2001].

Field-aligned L-mode EMIC waves are confined to frequency bands below each ion gyrofrequency, with a propagation “stop-band” (in which L-mode propagation is not allowed) between the cut-off frequency ω_{cut} and each heavy ion gyrofrequency. The location of ω_{cut} is controlled by the relative concentration of the heavy ions. Figure 1 gives an example of the dispersion properties of EMIC waves for realistic ion composition in the inner magnetosphere. Precise knowledge of the heavy ion composition is critical, since this strongly influences the phase speed of the wave (and hence the resonant particle energies) over the frequency range where waves are preferentially excited. For example, the presence of He^+ ions lowers the wave phase speed of L-mode waves in the band below the He^+ gyrofrequency compared to values for a single ion H^+ plasma. This lowers the ion cyclotron resonant energies and enhances the wave growth rate. As a consequence, the spectral intensity of EMIC waves is often enhanced in the frequency band between the He^+ and O^+ gyrofrequencies.

Although the growth rate of EMIC waves maximizes for field-aligned propagation, wave normal angles generally become oblique, as the waves propagate away from the source location in the highly non-uniform magnetospheric plasma (Section 3). Oblique propagation adds considerable complexity to the wave dispersion relation. Waves can change their dominant sense of polarization at the characteristic crossover frequencies, which correspond to the locations (Figure 1) where the R and L-mode waves have the same phase speed. The change in polarization allows L-mode waves, which are excited near the equator at frequencies above the crossover frequency ω_{cr} , to propagate across the “stop band” (as predominantly R-mode waves) during their propagation to higher latitude. This property, together with tunneling (section 3.2), is ultimately responsible for allowing some EMIC wave energy to reach the

ground, rather than being reflected at the cut-off frequencies.

Another important oblique wave propagation characteristic is the presence of the bi-ion frequency ω_{bi} (Figure 2), below which waves are allowed to propagate with k -vectors perpendicular to the magnetic field. The effect of the bi-ion frequency is analogous to the lower hybrid frequency on whistler propagation. During propagation to higher latitude, highly oblique EMIC waves can experience the equivalent of a magnetospheric reflection, and thus remain trapped in the magnetosphere, similar to magnetospherically reflected whistlers [e.g., *Thorne and Horne, 1994b; Bortnik et al., 2003*]. However, one important distinction in the propagation characteristics of these two waves is the location of the bi-ion frequency just above the gyrofrequency of each heavy ion. Because of the proximity to the heavy ion gyrofrequency, EMIC waves experience substantial cyclotron resonant absorption close to their reflection point [*Thorne and Horne, 1993*], while MR whistlers remain essentially undamped. An important consequence of EMIC absorption is the perpendicular heating of heavy ions at locations away from the equator (Section 4.1). Wave absorption near the bi-ion frequency also prevents significant wave power from returning to the equator and probably accounts for observations that the EMIC pointing flux is predominantly directed towards the Earth at locations well away from the equatorial source [*Fraser et al., 1996; Loto'aniu et al., 2005*]

1.3. Particle Resonance with EMIC Waves.

Magnetospheric particles can resonate with EMIC waves whenever the Doppler-shifted wave frequency (as viewed in the frame of reference of the particle) is equal to an integral multiple ($n = 0, \pm 1, \pm 2, \dots$) of the particle gyrofrequency, $\Omega = qB/m$:

$$\omega - k_{\parallel} v_{\parallel} = n \Omega / \gamma \quad (1)$$

where $\gamma = \{1 - (v/c)^2\}^{-1/2}$ is the relativistic factor and k_{\parallel} and v_{\parallel} are components of the wave propagation vector and particle velocity along the direction of the ambient magnetic field. During wave-particle interactions, there can be a net wave-particle exchange of momentum and energy leading to particle scattering and wave growth or damping.

1.3.1 Landau resonant interactions ($n=0$). When particles move along the field with a velocity equal to the parallel wave phase speed, particles experience a static wave electric field in their reference frame. Since the EMIC wave phase speed is generally well below the speed of light, Landau resonant energies lie in the thermal range (typically \sim few eV for electrons and a few keV for ions). Landau interactions usually lead to wave attenuation,

which is most significant for highly-oblique EMIC waves, due to the presence of a strong field-aligned component of the wave electric field [Thorne and Horne, 1992]. Landau damping of oblique EMIC waves by plasmaspheric electrons contributes to electron heating in the outer plasmasphere during storm conditions (Section 5.1) leading to a net heat flux into the atmosphere that is responsible for producing SAR arcs [Cornwall *et al.* 1971; Thorne and Horne, 1992].

1.3.2 Cyclotron resonance with ring current ions. Because EMIC waves occur at frequencies below the H^+ gyrofrequency, first order ($n = 1$) cyclotron resonance requires that H^+ ions move along the field in the opposite direction to the waves, causing an upward Doppler shift in frequency. Typical proton resonant energies lie in the ring current (5-50 keV) range. During the wave-particle interactions, anisotropic protons are preferentially scattered into the atmosphere and lose energy, providing a natural energy source for wave excitation (Section 2). EMIC waves can also interact with higher energy (>100 keV) ions and contribute to their loss from the radiation belts.

1.3.3 Cyclotron resonance with relativistic electrons. Extremely high-energy electrons can also resonate with EMIC waves. Because the waves are predominantly left-hand polarized, electrons must overtake the wave (reversing the apparent sense of polarization to R-mode) with a velocity sufficient to Doppler shift the wave frequency from below the ion gyrofrequency to the relativistic electron gyrofrequency. Such resonance can only occur for extremely high electron energy, and the minimum energy for resonance is highly sensitive to the plasma density, ion composition, and the wave spectral characteristics (Section 5.2). Nonetheless, EMIC waves can provide an important scattering loss for > 0.5 MeV electrons in localized regions just inside the plasmopause and within high-density dayside drainage plumes that form during storm conditions.

2. EMIC WAVE EXCITATION MECHANISMS

2.1. Convective Injection of Ring Current Ions.

Intensification of the large-scale convection electric field can lead to rapid injection of plasma sheet ions into the inner magnetosphere and the enhancement of the ring current. During the injection, ring current ions develop an anisotropic distribution with $T_{\text{perp}} > T_{\text{par}}$. For sufficiently large resonant ion flux, these anisotropic distributions are unstable to the cyclotron resonant excitation of electromagnetic ion cyclotron waves [e.g., Kennel and Petschek, 1966]. For a single ion plasma, peak wave growth occurs at a normalized frequency just below the condition for marginal stability, $(\omega/\Omega_+)_{\text{max}} = 1 - T_{\text{par}} / T_{\text{perp}}$. Above this

critical frequency, waves are cyclotron damped, while at low frequency, resonant energies become too high (and the resonant flux too low) to produce substantial amplification. Cyclotron resonant energies minimize at the equator for waves with propagation vectors directed along the ambient magnetic field [*Horne and Thorne, 1993, 1994; Thorne and Horne, 1997*]. The presence of heavy ions, such as He^+ and O^+ , can significantly influence the phase speed of EMIC waves, especially in the vicinity of the heavy ion gyrofrequencies (Figures 1, 2). As a consequence, the resonant ring current proton energies can be lowered, leading to enhanced wave growth, especially in the frequency band just below the He^+ gyrofrequency [*Gomberoff and Neira, 1983; Gendrin et al., 1984; Kozyra et al., 1984*]. The most intense EMIC waves observed in the magnetosphere are consequently found in two bands above and below the He^+ gyrofrequency.

Resonant ion energies are also lowered by the increase in plasma density inside the plasmopause [*Cornwall et al., 1970; Perraut et al., 1976*], and the guidance of EMIC waves by density gradients near the plasmopause can substantially enhance the net path integrated gain (Figure 3) as waves propagate across the equator [*Thorne and Horne, 1997*]. Kinetic ring current codes have been developed to simulate the injection and subsequent loss of ions from the storm-time ring current [e.g., *Jordanova et al., 2003*]. All of the important physical processes can be incorporated into such codes and model results are in good agreement with satellite observation. In particular, the spatial regions for preferential excitation of EMIC waves have been simulated with the RAM code (e.g., Figure 4), based on a detailed modeling of the spatial distribution of ring current ions and their pitch-angle anisotropy [*Jordanova et al., 1998, 2001a,b*] and shown to agree well with the statistical spatial distribution of waves observed on satellites [e.g., *Erlandson and Ukhorskiy, 2001, Meredith et al., 2003*]. Although charge exchange and Coulomb scattering are the dominant global loss processes for ring current decay in the recovery phase of a storm, scattering by EMIC waves can cause intense precipitation into the atmosphere, in spatially confined regions where the waves are present (Figure 4). Such wave-induced losses remove about 10% of the ions injected into the storm-time ring current [*Jordanova, 2005*]

2.2. Solar Wind Compression Events.

Sudden increases in the dynamic pressure of the solar wind can cause an increase in the thermal anisotropy of trapped ring current ions, which enhances the growth rate of EMIC waves [*Olson and Lee, 1983*]. Analysis of particle and field data on the AMPTE/CCE satellite in the day-side magnetosphere indicates that enhancements in solar wind pressure can excite EMIC waves driven by changes in the energetic proton population [*Anderson and Hamil-*

ton, 1993]. Since the early 1960's, it has been noted that micro-pulsations observed near noon on ground-based magnetometers are associated with sudden impulses. The excitation Pc 1 band waves, observed both on the ground, and on the Polar spacecraft, has recently been directly associated with solar wind pressure pulses [Arnoldy *et al.*, 2005], which cause an enhancement in the energetic ring current proton flux in the direction transverse to the magnetic field.

2.3. Modulation of EMIC waves by ULF oscillations.

A third mechanism for the excitation of magnetospheric EMIC waves involves changes in the distribution function of the resonant ion population caused by large amplitude ULF oscillations [Rasinkangas and Mursala, 1998; Fraser, 2006]. Such ULF waves, which are commonly present during geomagnetically active periods, can modulate the flux and pitch-angle anisotropy of energetic ions [e.g., Coroniti and Kennel, 1970] and thus trigger bursts of EMIC wave amplification.

3. EMIC PROPAGATION CHARACTERISTICS

3.1. EMIC Wave Polarization and Poynting Flux.

The direction of EMIC wave propagation, and the wave polarization have been determined using triaxial magnetic field data from the CRRES satellite, together with two orthogonal components of the wave electric field [Fraser *et al.*, 1996]. For most wave events analyzed, the Poynting flux was predominantly directed away from the equator. The only exceptions occurred when CRESS was located close to the equator. The results were interpreted as evidence for an equatorial source, due to cyclotron instability, with minimal wave reflection from the ionosphere (or as discussed below at the bi-ion frequency). A more recent detailed analysis by Loto'aniu *et al.* [2005] has confirmed the concept of a broad equatorial source region, with unidirectional energy propagation away from the equator above 11° latitude. These observations are inconsistent with the bouncing wave packet model [Jacobs and Watanabe, 1963] and instead suggest that EMIC wave excitation occurs during a single transit of the wave across the equator.

3.2. Ray Trace Modeling of EMIC Waves.

Although the source location for EMIC waves is thought to be near the equatorial region, the waves are able to propagate for large distances and may ultimately reach the ground. Ray tracing codes have been developed to follow the propagation of wave energy in the heterogeneous magnetospheric environment. Such codes use the eikonal approximation of geometrical optics [e.g., Budden, 1985] to

follow the wave group velocity for a specified magnetic field and plasma density model. Due primarily to the curvature of the Earth's magnetic field, the wave propagation vector tends to become oblique, as waves travel away from an equatorial source towards the Earth (Figure 3). However, even for highly-oblique propagation, the group velocity of EMIC waves remains remarkably aligned along the ambient magnetic field, except in the vicinity of the bi-ion frequency (Figure 2), where ray propagation perpendicular to the field can occur. Under the standard geometrical optics approximation, highly oblique EMIC waves, traveling towards the Earth, are predicted to reflect close to the location where their frequency becomes equal to the bi-ion frequency [Rauch and Roux, 1982], and thus remain trapped in the magnetosphere. This is analogous to the magnetospheric reflection of lightning-generated whistlers at the lower hybrid frequency [Kimura, 1966; Thorne and Kennel, 1967]. The concentration of He^+ and O^+ ions, which control the bi-ion frequency, can thus influence the ability of EMIC waves to propagate to high latitude, and ultimately reach the ground. However, the approximations employed by ray tracing codes are invalid in the vicinity of the bi-ion reflection location. Waves may mode-convert and tunnel through the critical region when the heavy ion concentration is low, thus allowing wave energy to propagate on towards the Earth. This, presumably, is the reason why some wave energy reaches the ground. Those waves that do reflect experience significant cyclotron resonant absorption near the reflection point [Thorne and Horne, 1993; Horne and Thorne, 1997]. Consequently, little wave energy is able to return to the equatorial region, thus accounting for the Poynting flux observations discussed above.

4. RESONANT INTERACTION WITH IONS

4.1. Thermal Ion Heating

Anderson and Fuselier [1994] and Fuselier and Anderson [1996] have presented compelling evidence for a correlation between periods of enhanced EMIC wave activity and thermal He^+ ions that are heated to energies near 20 eV, in the direction perpendicular to the magnetic field. He^+ observations taken near the equator exhibited a conic distribution, which according to adiabatic transport, are indicative of perpendicular heating at magnetic latitudes as high as 40° . Using a plasma model based on AMPTE observations, the HOTRAY code [Horne, 1989] has been used by Horne and Thorne [1997] to study the equatorial growth of EMIC waves at $L = 7$ in the band above the He^+ gyrofrequency. The simulations indicate EMIC wave gain in excess of 60 db during a single pass through the equatorial growth region, thus accounting for the large occurrence of such waves in the outer dayside magnetosphere [Ander-

son *et al.*, 1996]. Furthermore, as the waves propagate to higher latitude they become highly oblique and are eventually absorbed (by He^+ cyclotron resonance) near the bi-ion frequency, leading to high-latitude transverse heating of He^+ and the formation of the conic distributions observed by AMPTE near the equator.

EMIC waves excited in the frequency range below the He^+ gyrofrequency can be absorbed by O^+ ions, either at the bi-ion frequency or at the second harmonic of the O gyro-frequency [Thorne and Horne, 1994a], leading to O^+ heating. This process is expected to be most effective under storm conditions when the magnetospheric composition of O^+ is enhanced.

4.2. Scattering of Ring Current Ions

Quasi-linear theory describes the effect of the wave fields on the energetic particle distributions as a diffusive process. Diffusion coefficients considering resonant interactions with ion cyclotron and whistler waves in an electron-proton medium were first derived by Lyons [1974], while Jordanova *et al.* [1996] first derived the diffusion coefficients for a multi-component plasma. For most of the wave frequencies of interest, ring current ions in a multi-component plasma resonate at lower parallel energies than ions in an electron-proton plasma, for a given harmonic value. As a result, the ion diffusion lifetimes significantly decrease at low energies (~ 10 to 100 keV) in a multi-component, as compared to an electron-proton plasma, causing stronger wave-induced losses of ring current ions [Jordanova *et al.*, 1996].

The PADIE code [Glauert and Horne, 2005] has recently been developed to evaluate the quasi-linear rate of pitch-angle scattering and energy diffusion for particles resonant with any specified distribution of plasma wave in the magnetosphere. The computations require a model for the density and magnetic field and the spectral intensity of plasma waves along a field line. Figure 5 shows bounce-averaged diffusion rates of energetic ions for a realistic distribution of EMIC waves, assuming a conservative wide band amplitude of 1 nT. Wave energy is distributed over a Gaussian distribution of frequencies, with peak power spectral intensity at $3 \Omega_{\text{O}^+}$, a bandwidth of $0.8 \Omega_{\text{O}^+}$, and upper and lower cut-offs at $2.2 \Omega_{\text{O}^+}$ and $3.8 \Omega_{\text{O}^+}$ respectively. Waves are assumed to have a Gaussian distribution of propagation vectors, centered on the magnetic field with an angular spread of 15° , and is assumed to be confined within 20 degrees of the equator. A dipole magnetic field model, with constant density along the field and an equatorial ratio of $f_{\text{pc}}/f_{\text{ce}} = 20$ (to simulate conditions near $L=4$ just inside the plasmopause), is used to evaluate the bounce averages. The results, shown in Figure 5, indicate that 3-10 keV ring current ions experience pitch-angle scattering

near the loss cone, $D_{\alpha\alpha} \sim 3 \times 10^{-5} \text{ rad}^2/\text{s}$. The scattering of higher-energy ions is considerably slower, becoming negligible for energies above 300 keV. Corresponding ion lifetimes due to scattering loss into the atmosphere can be obtained by numerical solution of the Fokker-Plank equation [Schulz and Lanzerotti, 1974], using the computed bounce-averaged diffusion rates [e.g., Thorne *et al.*, 2005a]. Since EMIC waves are spatially confined (e.g., Figure 4), the computed lifetimes must also be scaled to account for the fraction of the ion drift orbit (typically 1-10 %) spent in resonance with the waves. Diffusion rates also scale in direct proportion to the power in the wave, and would therefore be two orders of magnitude larger than indicated, if the wave amplitude were 10 nT (comparable to peak values observed during storm conditions). Lifetimes for ring current ions during storm conditions should therefore lie in the range between a few hours at 10 keV and a day at 100 keV. Scattering of higher-energy ions would be enhanced, if significant wave power extended to latitudes above 20° .

Simulations of EMIC wave excitation with the RAM code (Figure 4) indicate preferential net wave gain along the dusk-side plasmopause and within storm-time plasma plumes [Spasojevic *et al.*, 2003], due to the lowering of ion resonant energy associated with enhanced plasma density [Cornwall *et al.*, 1970]. The most intense ion precipitation occurs in localized regions associated with the storm-time plumes, as recently observed by Spasojevic *et al.*, [2004].

5. RESONANT INTERACTION WITH ELECTRONS

5.1 Landau Damping by Thermal Electrons

Owing to the low phase speed of EMIC waves, Landau resonant energies with electrons are in the thermal range near a few eV. Landau resonant absorption becomes important when EMIC waves propagate at large wave normal angles, due to the large parallel electric field of the wave [Thorne and Horne, 1992]. EMIC waves excited by ring current ions just inside the plasmopause can therefore transfer energy to the thermal electron population in the outer plasmasphere during storm conditions, thus contributing to the downward heat flux required to account for SAR arcs [Cornwall *et al.*, 1971].

5.2 Scattering of Relativistic Electrons

Relativistic electrons are also able to interact with EMIC waves via the Doppler-shifted cyclotron resonance. Since the waves are predominantly left-hand polarized, electrons must overtake the wave with a velocity sufficient to cause a Doppler-shift in frequency from below the ion gyro-frequency up to the relativistic gyro-frequency of the elec-

trons. This is only possible at extremely high energies, as initially discussed by *Thorne and Kennel* [1971]. However, since EMIC wave intensities are considerably larger than other waves (such as VLF whistler-mode emissions), which interact with such electrons, scattering can be very rapid, especially during the main phase of a magnetic storm. Initial estimates for scattering rates by *Thorne and Kennel* [1971] and *Lyons and Thorne* [1972], for a single ion H^+ plasma, suggested relativistic electron lifetimes less than an hour. Recently, electron diffusion rates have been evaluated for a realistic multi-ion plasma [*Albert, 2003; Summers and Thorne, 2003*], and CRRES wave observation have been used to compute the minimum electron energy for resonance [*Meredith et al., 2003*].

In Figure 6 we show the bounce averaged pitch-angle and energy diffusion rates for energetic electrons, using the same wave and plasma properties adopted for the ion calculations in Figure 5. For the chosen wave properties, the minimum energy for electron cyclotron resonance is just below 1 MeV. Energy diffusion is clearly negligible in agreement with previous assessments [e.g., *Summers et al. 1998*]. However, relativistic electron pitch-angle scattering near the loss cone is two orders of magnitude higher than corresponding scattering rates for 10 keV ring current ions. Such electrons should be removed rapidly (within an hour) from the radiation belts at the onset of a storm, once EMIC waves are excited by the injection of ring current ions. This could account for the intense high-energy X-ray bursts reported by *Millan et al.* [2002]. However, electron scattering by EMIC waves is only effective at pitch-angles less than 40° - 60° , so other scattering processes (such as scattering by whistler-mode chorus [*Thorne et al., 2005b*] and hiss [*Abel and Thorne, 1998*]) are required to remove relativistic electrons trapped near the equator. Because the scattering rate from these other waves is much slower (due to the weaker wave amplitudes) the net removal time for trapped outer zone relativistic electrons is substantially longer than an hour, but is probably less than a day [e.g., *Albert, 2003*]. Further quantification of the net loss process needs to be undertaken, but scattering by EMIC and other storm-time waves is a potential candidate to explain the observed sudden dropout [*Onsager et al., 2002; Green et al., 2004*] of relativistic electron flux at the onset of enhanced geomagnetic activity.

6. CONCLUDING REMARKS

EMIC waves are able to resonate with magnetospheric ions and electrons over a broad range of energies. The interactions lead to particle pitch-angle scattering and energy diffusion. The source of EMIC wave excitation is provided by the anisotropic pitch-angle distribution of ring current ions. EMIC waves are consequently enhanced during disturbed conditions, particularly during the onset of a mag-

netic storm. Wave energy is subsequently transferred to other resonant particles, causing the heating of thermal magnetospheric ions and electrons. Resonant relativistic electrons also experience rapid pitch-angle scattering and loss to the atmosphere. In high-density regions (such as the plasmasphere or storm-time drainage plumes), minimum electron energies can fall to values less than one MeV. Relativistic electron scattering loss during the main phase of a storm, when ions are rapidly injected into the ring current leading to intense EMIC amplification, is sufficiently rapid to dominate over anticipated acceleration processes. Consequently, there is a net loss of relativistic outer radiation belt electrons at the onset of a storm. Relativistic electron precipitation at MeV energies is expected to occur along the dusk-side plasmopause and with drainage plumes.

In low-density regions exterior to the plasmopause, resonant electron energies generally lie above 10 MeV [Meredith *et al.*, 2003]. Scattering of such energetic electrons in the outer radiation belt by EMIC waves inhibits the build-up of an ultra-relativistic electron population in the Earth's radiation belts. As a consequence, fluxes drop dramatically above a few MeV, and extremely relativistic electrons (>10 MeV) are rarely produced in the Earth's outer radiation belt, even under disturbed conditions. This contrasts sharply with the Jovian middle magnetosphere, where ultra-relativistic electrons are constantly present and pose a hazard to spacecraft. Inward radial diffusion of such energetic electrons (in the absence of significant scattering loss) ultimately leads to the synchrotron radiation from the inner Jovian radiation belts [Bolton *et al.*, 2004]. Interestingly, the rapid removal of relativistic electrons from the Earth's outer radiation belt, due to scattering by EMIC and other waves, probably accounts for the absence of significant synchrotron radiation from the terrestrial radiation belts.

Acknowledgments. The work was supported by NASA grants NAG5-11922, NAG5-13512, NNG04GN44G and NSF grant ATM 0402615.

REFERENCES

- Abel, B., and R. M. Thorne (1998), Electron scattering loss in Earth's inner magnetosphere, 1, Dominant physical processes, *J. Geophys. Res.*, *103*, 2385.
- Albert, J. M. (2003), Evaluation of quasi-linear diffusion coefficients for EMIC waves in a multi-species plasma, *J. Geophys. Res.*, *108*(A6), 1249, doi:10.1029/2002JA009792.
- Anderson, B. J., R. E. Erlandsen, and L. J. Zanetti (1992), A statistical study of Pc1-2 magnetic pulsations in the equatorial magnetosphere 1. Equatorial occurrence distributions, *J. Geophys. Res.*, *97*, 3075.
- Anderson, B. J., and D. C., Hamilton (1993), Electromagnetic ion cyclotron waves stimulated by modest magnetospheric compressions, *J. Geophys. Res.*, *98*, 11,369.

- Anderson, B. J., and Fuselier (1994), Response of thermal ions to electromagnetic ion cyclotron waves, *J. Geophys. Res.*, *99*, 19,413.
- Arnoldy, R. L. et al. (2005), Pc1 waves and associated unstable distributions of magnetospheric protons observed during a solar wind pressurer pulse, *J. Geophys. Res.*, *110*, A07229, doi:10.1029/2005JA011041.
- Bolton, S. J., R. M. Thorne, S. Bourdarie, B. H. Mauk, and I. de Pater (2004), Jupiter's inner radiation belts, in *Jupiter: The Planet, Satellites, and Magnetosphere*, edited by F. Bagenal, T. Dowling, and W. McKinnon, pp. 671-688, Cambridge University Press.
- Bortnik J., U. S. Inan, and T. F. Bell (2003), Frequency-time spectra of magnetospherically reflecting whistlers in the plasmasphere, *J. Geophys. Res.*, *108*(A1), 1030, doi:10.1029/2002JA009387.
- Braysy, T., K. Mursala, and G. Markland (1998), Ion cyclotron waves during a great magnetic storm observed by Freja double-probe electric field instrument, *J. Geophys. Res.*, *103*, 4145.
- Budden, K. G. (1985), *The Propagation of Radio Waves*, Cambridge University Press.
- Cornwall, J. M., F. W. Coroniti and R. M. Thorne (1970), Turbulence loss of ring current protons, *J. Geophys. Res.*, *75*, 4699.
- Cornwall, J. M., F. V. Coroniti, and R. M. Thorne (1971), Unified theory of SAR arc formation at the plasmapause, *J. Geophys. Res.*, *76*, 4428.
- Coroniti, F.V., and C.F. Kennel (1970), Electron precipitation pulsations, *J. Geophys. Res.*, *75*, 1279.
- Erlanson, R. E., and A. J. Ukhorskiy (2001), Observations of electromagnetic ion cyclotron waves during geomagnetic storms: wave occurrence and pitch angle scattering, *J. Geophys. Res.*, *106*, 3883.
- Fraser, B. J., T. M. Loto'aniu, and H. J. Singer (2006), Electromagnetic ion cyclotron waves in the magnetosphere, in *Magnetospheric ULF Waves. Monogr. Ser.*, vol. XXX, edited by K. Takahashi, B. Lysak, R. Denton, and P. Chi, pp XXX, AGU, Washington, D. C.
- Fraser, B. J., H. J. Singer, W. J. Hughes, W. J. Wygant, R. R. Anderson, and Y. D. Hu (1996), CRRES Poynting vector observations of electromagnetic ion-cyclotron waves near the plasmapause, *J. Geophys. Res.*, *101*, 15,331.
- Fuselier, S. A., and B. J. Anderson (1996), Low energy He⁺ and H⁺ distributions and proton cyclotron waves in the afternoon equatorial magnetosphere, *J. Geophys. Res.*, *101*, 13,255.
- Gendrin, R., M. Ashour-Abdalla, Y. Omura, and K. Quest (1984), Linear analysis of ion cyclotron interactions in a multicomponent plasma, *J. Geophys. Res.*, *89*, 9119.
- Glauert, S. A., and R. B. Horne (2005), Calculation of pitch-angle and energy diffusion coefficients with the PADIE code, *J. Geophys. Res.*, *110*, A04206, doi:10.1029/2004JA010851.
- Gomberoff, L., and R. Neira (1983), Convective growth rate of ion cyclotron waves in a H⁺ - He⁺ - O⁺ plasma, *J. Geophys. Res.*, *88*, 2170.
- Green, J. C., T. G. Onsager, T. P. O'Brien, and D. N. Baker (2004), Testing loss mechanisms capable of rapidly depleting relativistic electron flux in the Earth's outer radiation belt, *J. Geophys. Res.* *109*, A12211, doi:10.1029/2004JA010579.
- Horne, R. B. (1989), Path-integrated growth of electrostatic waves: the generation of terrestrial myriametric radiation, *J. Geophys. Res.*, *94*, 8895.

- Horne, R. B., and R. M. Thorne (1993), On the preferred source location for convective amplification of ion-cyclotron waves, *J. Geophys. Res.*, *98*, 9,233.
- Horne, R. B., and R. M. Thorne (1994), Convective instabilities of electromagnetic ion cyclotron waves in the outer magnetosphere, *J. Geophys. Res.*, *99*, 17,259.
- Horne, R. B., and R. M. Thorne (1997), Wave heating of He⁺ by electromagnetic ion-cyclotron waves in the outer magnetosphere: Heating near the H⁺–He⁺ bi-ion resonance frequency, *J. Geophys. Res.*, *102*, 14,155.
- Horne, R. B., R. M. Thorne, S. A. Glauert, J. M. Albert, N. P. Meredith, and R. R. Anderson (2004), Timescales for radiation belt electron acceleration by whistler mode chorus waves, *J. Geophys. Res.*, *111*, A03225, doi:10.1029/2004JA010811.
- Jacobs, J. A., and T. Watanabe (1963), Trapped charged particles as the source of short period geomagnetic pulsations, *Planet. Space Sci.*, *11*, 869.
- Jordanova, V. K. (2005), Sources, transport, and losses of energetic particles during geomagnetic storms, in *The Inner Magnetosphere: Physics and Modeling*, Geophys. Monogr. Ser., vol. 155, ed. by T. I. Pulkkinen, N. A. Tsyganenko, and R. H. W. Friedel, p 9, AGU, Washington, D. C.
- Jordanova, V. K., J. U. Kozyra, and A. F. Nagy (1996), Effects of heavy ions on the quasi-linear diffusion coefficients from resonant interactions with EMIC waves, *J. Geophys. Res.*, *101*, 19,771.
- Jordanova, V. K., et al. (1998), Effect of wave-particle interactions on ring current evolution for January 10-11, 1997: Initial results, *Geophys. Res. Lett.*, *25*, 2971.
- Jordanova, V. K., C. J. Farrugia, R. M. Thorne, G. V. Khazanov, G. D. Reeves, and M. F. Thomsen (2001), Modeling ring current proton precipitation by EMIC waves during the May 14-16, 1997 storm, *J. Geophys. Res.*, *106*(A1), 7.
- Jordanova, V. K., A. Boonsiriseth, R. M. Thorne, and Y. Dotan, Ring current asymmetry from global simulations using a high-resolution electric field model (2003), *J. Geophys. Res.*, *108*(A12), 1443, doi:10.1029/2003JA009993.
- Kennel, C. F., and H. E. Petschek (1966), Limit on stably trapped particle fluxes, *J. Geophys. Res.*, *71*, 1.
- Kim, H.-J., and A. A. Chan (1997), Fully adiabatic changes in storm time relativistic electron fluxes, *J. Geophys. Res.*, *102*, 22,107.
- Kimura, I (1966), Effects of ions on whistler-mode ray tracing, *Radio Sci.*, *1*, 269.
- Kozyra, J. V., T. E. Cravens, A. F. Nagy, E. G. Fontheim, and R. S. Ong, (1984), Effects of energetic heavy ions on electromagnetic ion cyclotron wave generation in the plasmopause region, *J. Geophys. Res.*, *89*, 2217.
- Loto'aniu, T. M., B. J. Fraser, and C. L. Walters (2005), Propagation of electromagnetic ion cyclotron waves energy in the magnetosphere, *J. Geophys. Res.*, *110*, A07214, doi:10.1029/2004JA010816.
- Lorentzen, K. R., M. P. McCarthy, G. K. Parks, J. E. Float, R. M. Millan, D. M. Smith, R. P. Lin, and J. P. Treilhou (2000), Precipitation of relativistic electrons by interaction with electromagnetic ion cyclotron waves, *J. Geophys. Res.*, *105*, 5381.
- Lyons, L. R., and R. M. Thorne (1972), Parasitic pitch angle diffusion of radiation belt particles by ion cyclotron waves, *J. Geophys. Res.*, *77*, 5608.
- Meredith, N. P., R. M. Thorne, R. B. Horne, D. Summers, B. J. Fraser, and R. R. Anderson (2003), Statistical analysis of rela-

- tivistic electron energies for cyclotron resonance with EMIC waves observed on CRRES, *J. Geophys. Res.*, *108*(A6), 1250, doi:10.1029/2002JA009700.
- Millan, R. M., R. P. Lin, D. M. Smith, K. R. Lorentzen, and M. P. McCarthy (2002), X-ray observations of MeV electron precipitation with a balloon-borne germanium spectrometer, *Geophys. Res. Lett.*, *29*(24), 2194, doi:10.1029/2002GL015922.
- Olson, J. V., and L. C. Lee (1983), Pc 1 wave generation by sudden impulses, *Space Sci.*, *31*, 295.
- Onsager, T. G., G. Rostoker, H. J. Kim, T. Obara, H. J. Singer, and C. Smith (2002), Radiation belt electron dropouts: Local time, radial, and particle energy dependence, *J. Geophys. Res.*, *107*(A7), 1382, doi:10.1029/2001JA000187.
- Perault, S., R. Gendrin, and A. Roux (1976), Amplification of ion cyclotron waves for various typical radial profiles of magnetospheric parameters, *J. Atmos. Terr. Phys.*, *38*, 1191.
- Rasinkangas, R., and K. Mursula (1998), Modulation of magnetospheric EMIC waves by Pc3 pulsations of upstream origin, *Geophys. Res. Lett.*, *25*, 869.
- Rauch, J. L., and A. Roux (1982), Ray tracing of ULF waves in a multi-component magnetospheric plasma: Consequences for the generation mechanism of ion cyclotron waves, *J. Geophys. Res.*, *87*, 8191.
- Roederer, J. G. (1970), *Dynamics of Geomagnetically Trapped Radiation*, Springer-Verlag, New York.
- Schulz, M., and L. Lanzerotti (1974), *Particle Diffusion in the Radiation Belts*, Springer, New York.
- Spasojevic, M., J. Goldstein, D. L. Carpenter, U. S. Inan, B. R. Sandel, M. B. Moldwin, and B. W. Reinisch (2003), Global response of the plasmasphere to a geomagnetic disturbance, *J. Geophys. Res.*, *108*(A9), 1340, doi:10.1029/2003JA009987.
- Spasojevic, M., H. U. Frey, M. F. Thomsen, S. A. Fuselier, S. P. Gary, B. R. Sandel, and U. S. Inan (2004), The link between a detached subauroral proton arc and a plasmaspheric plume, *Geophys. Res. Lett.*, *31*, L04803, doi:10.1029/2003GL018389.
- Summers D., and R. M. Thorne (2003), Relativistic electron pitch-angle scattering by electromagnetic ion cyclotron waves during geomagnetic storms, *J. Geophys. Res.*, *108*(A4), 1143, doi:10.1029/2002JA009489.
- Summers, D., R. M. Thorne, and F. Xiao (1998), Relativistic theory of wave-particle resonant diffusion with application to electron acceleration in the magnetosphere, *J. Geophys. Res.*, *103*, 20,487.
- Thorne, R. M., and C. F. Kennel (1967), Quasi-trapped VLF propagation in the outer magnetosphere, *J. Geophys. Res.*, *72*, 857.
- Thorne, R. M., and C. F. Kennel (1971), Relativistic electron precipitation during magnetic storm main phase, *J. Geophys. Res.*, *76*, 4446.
- Thorne, R. M., and R. B. Horne (1992), The contribution of ion-cyclotron waves to electron heating and SAR-arc excitation near the storm-time plasmapause, *Geophys. Res. Lett.*, *19*, 417.
- Thorne, R. M., and R. B. Horne (1993), Cyclotron absorption of ion-cyclotron waves at the bi-ion frequency, *Geophys. Res. Lett.*, *20*, 317.
- Thorne, R. M., and R. B. Horne (1994a), Energy transfer between energetic ring current H^+ and O^+ by electromagnetic ion-cyclotron waves, *J. Geophys. Res.*, *99*, 17,275.
- Thorne, R. M., and R. B. Horne (1994b), Landau damping of magnetospherically reflected whistlers, *J. Geophys. Res.*, *99*, 17,249.

Thorne, R. M., and R. B. Horne (1997), Modulation of electromagnetic ion cyclotron instability due to interaction with ring current O^+ during geomagnetic storms, *J. Geophys. Res.*, *102*, 14155.

Thorne, R. M., R. B. Horne, S. A. Glauert, N. P. Meredith, Y. Y. Shprits, D. Summers, and R. R. Anderson (2005a), The influence of wave-particle interactions on relativistic electron dynamics during storms, in *Inner Magnetosphere Interactions: New Perspectives from Imaging*, *Geophys. Monogr. Ser.*, vol. 159, edited by James L. Burch, Michael Schulz, and Harlan Spence, pp 101-112, AGU, Washington, D. C..

Thorne R. M., T. P. O'Brien, Y. Y. Shprits, D. Summers, and R. B. Horne (2005b), Timescale for MeV electron microburst loss during geomagnetic storms, *J. Geophys. Res.*, *110*, A09202, doi:10.1029/2004JA010882.

J. Bortnik, Department of Atmospheric and Oceanic Sciences, University of California, 7127 MS, Box 951565, Los Angeles, CA 90095-1565, USA.

S. Glauert, British Antarctic Survey, Natural Environment Research Council, Madingley Road, Cambridge, CB3 0ET, UK.

R. B. Horne, British Antarctic Survey, Natural Environmental Research Council, Madingley Road, Cambridge, CB3 0ET, UK.

V. K. Jordanova, Space Science Center, University of New Hampshire, 410 Morse Hall, 39 College Road, Durham. NH 03824, USA

R. M. Thorne, Department of Atmospheric and Oceanic Sciences, University of California, 7127 MS, Box 951565, Los Angeles, CA 90095-1565, USA.

FIGURE CAPTIONS

Figure 1. The dispersion relation for right (R) and left (L) hand polarized EMIC waves with propagation vectors along the magnetic field in a multi-ion magnetospheric plasma composed of 70% H⁺, 20% He⁺, and 10% O⁺. The phase speed of right and left hand polarized waves become equal at the two cross over frequencies ω_{cr} , allowing a change of polarization for different mode waves during propagation in the magnetosphere [Horne and Thorne, 1993].

Figure 2. The dispersion relation for EMIC waves propagating at 90° to the ambient magnetic field for the same ion composition in Figure 1. Perpendicular propagation (and magnetospheric reflection) of mode 4 and 5 waves only becomes possible for frequencies below each bi-ion frequency ω_{bi} [Horne and Thorne, 1993].

Figure 3. An example of EMIC wave amplification with the HOTRAY code [Thorne and Horne, 1997] showing the ray path (a), path integrated gain (b), and the change in wave normal angle (c) and normalized frequency (d) along the ray. Waves launched from below the equator are partially guided by the gradient in density associated with the plasmopause. Strongest gain occurs while the waves are field-aligned and damping sets in at higher latitude.

Figure 4. RAM code simulations of the excitation of EMIC waves, plasmaspheric density, and ion precipitation flux (20-100 keV) during a large geomagnetic storm in October, 2001. The ion precipitation increases by more than an order of magnitude when EMIC wave scattering is included, within regions of strong EMIC wave excitation along the duskside plasmopause and dayside drainage plumes.

Figure 5. PADIE computations of pitch-angle and energy diffusion rates for energetic ring current H⁺ ions. Bounce-averaged results are shown for 3 keV (solid), 10 keV (dotted), 30 keV (dashed), 100keV (dot-dashed), and 300 keV (dot dot dot dashed), resonant with EMIC waves below the He⁺ gyrofrequency.

Figure 6. PADIE code computations of pitch-angle and energy diffusion rates for relativistic electrons (1 MeV, solid; 2 MeV, dotted; 5 MeV dashed; and 10 MeV, dot dashed), resonant with EMIC waves below the He⁺ gyrofrequency.

Figure 1. The dispersion relation for right (R) and left (L) hand polarized EMIC waves with propagation vectors along the magnetic field in a multi-ion magnetospheric plasma composed of 70% H⁺, 20% He⁺, and 10% O⁺. The phase speed of right and left hand polarized waves become equal at the two cross over frequencies ω_{cr} , allowing a change of polarization for different mode waves during propagation in the magnetosphere [Horne and Thorne, 1993].

Figure 2. The dispersion relation for EMIC waves propagating at 90° to the ambient magnetic field for the same ion composition in Figure 1. Perpendicular propagation (and magnetospheric reflection) of mode 4 and 5 waves only becomes possible for frequencies below each bi-ion frequency ω_{bi} [Horne and Thorne, 1993].

Figure 3. An example of EMIC wave amplification with the HOTRAY code [Thorne and Horne, 1997] showing the ray path (a), path integrated gain (b), and the change in wave normal angle (c) and normalized frequency (d) along the ray. Waves launched from below the equator are partially guided by the gradient in density associated with the plasmopause. Strongest gain occurs while the waves are field-aligned and damping sets in at higher latitude.

Figure 4. RAM code simulations of the excitation of EMIC waves, plasmaspheric density, and ion precipitation flux (20-100 keV) during a large geomagnetic storm in October, 2001. The ion precipitation increases by more than an order of magnitude when EMIC wave scattering is included, within regions of strong EMIC wave excitation along the duskside plasmopause and dayside drainage plumes.

Figure 5. PADIE computations of pitch-angle and energy diffusion rates for energetic ring current H⁺ ions. Bounce-averaged results are shown for 3 keV (solid), 10 keV (dotted), 30 keV (dashed), 100keV (dot-dashed), and 300 keV (dot dot dot dashed), resonant with EMIC waves below the He⁺ gyrofrequency.

Figure 6. PADIE code computations of pitch-angle and energy diffusion rates for relativistic electrons (1 MeV, solid; 2 MeV, dotted; 5 MeV dashed; and 10 MeV, dot dashed), resonant with EMIC waves below the He⁺ gyrofrequency.

RADIATION BELT INTERACTION WITH EMIC WAVES

RADIATION BELT INTERACTION WITH EMIC WAVES

RADIATION BELT INTERACTION WITH EMIC WAVES

RADIATION BELT INTERACTION WITH EMIC WAVES

RADIATION BELT INTERACTION WITH EMIC WAVES

RADIATION BELT INTERACTION WITH EMIC WAVES

RADIATION BELT INTERACTION WITH EMIC WAVES

RADIATION BELT INTERACTION WITH EMIC WAVES

RADIATION BELT INTERACTION WITH EMIC WAVES

RADIATION BELT INTERACTION WITH EMIC WAVES

THORNE ET AL.

THORNE ET AL.

THORNE ET AL.

THORNE ET AL.

THORNE ET AL.

THORNE ET AL.

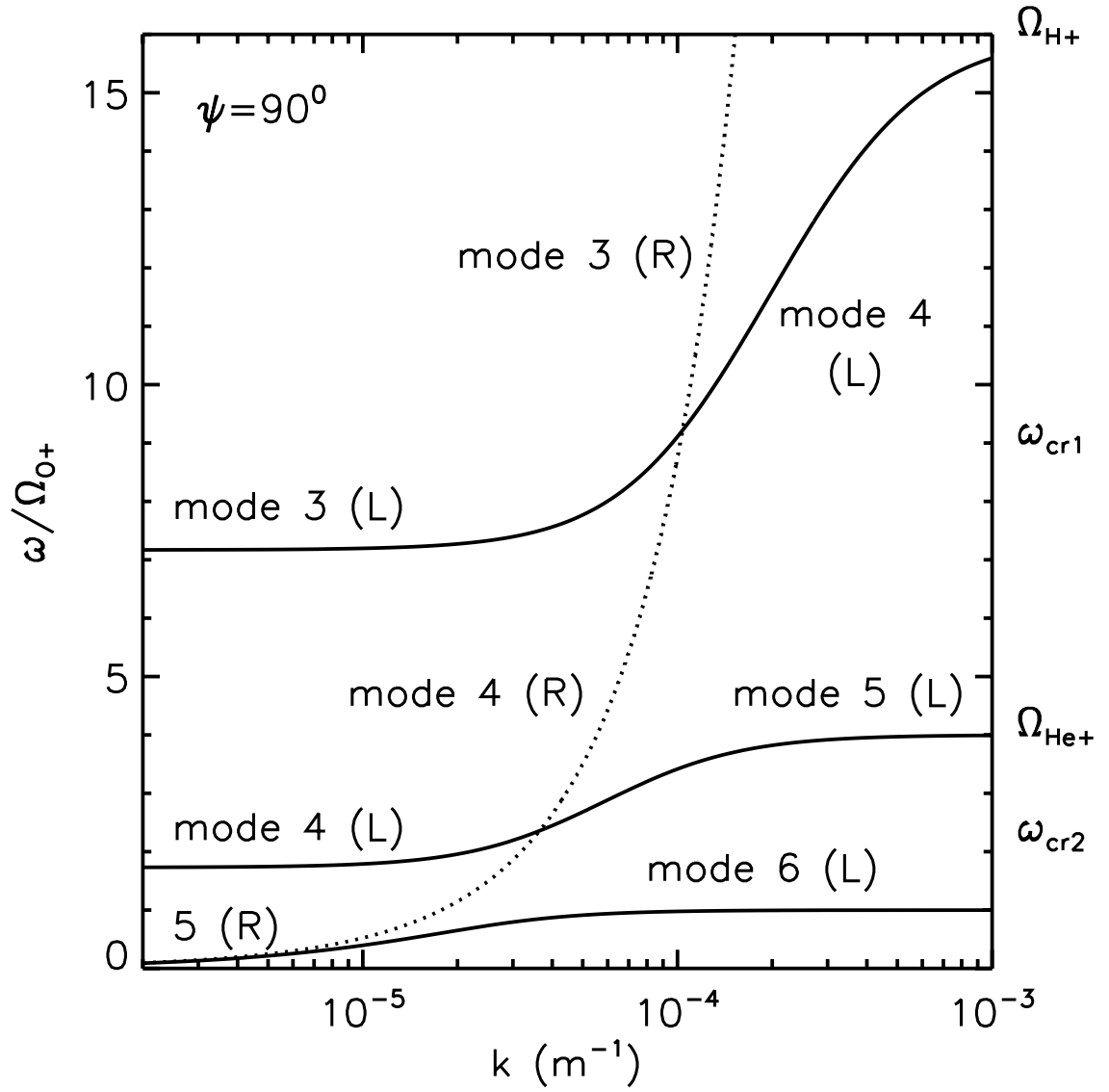
THORNE ET AL.

THORNE ET AL.

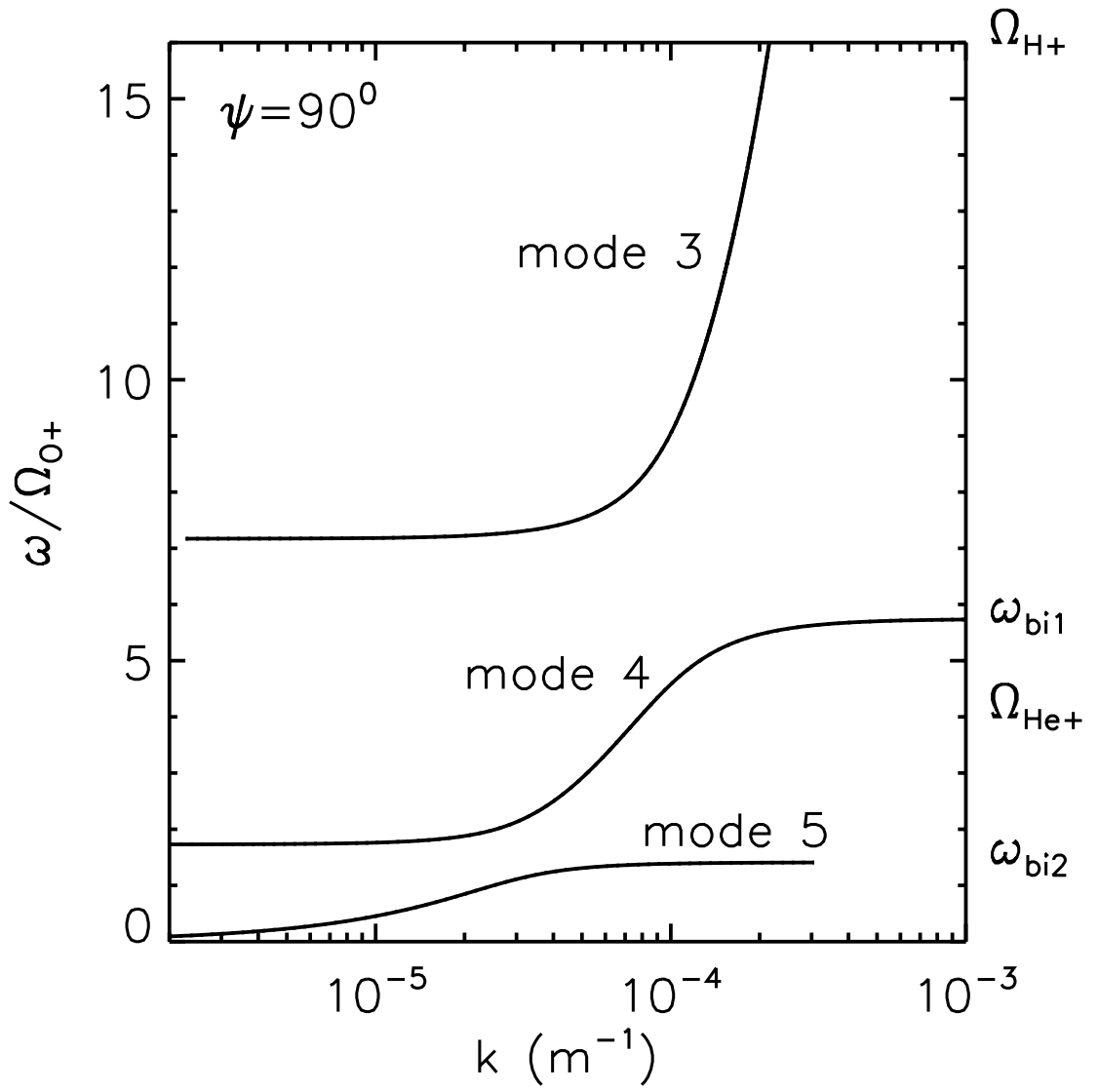
THORNE ET AL.

THORNE ET AL.

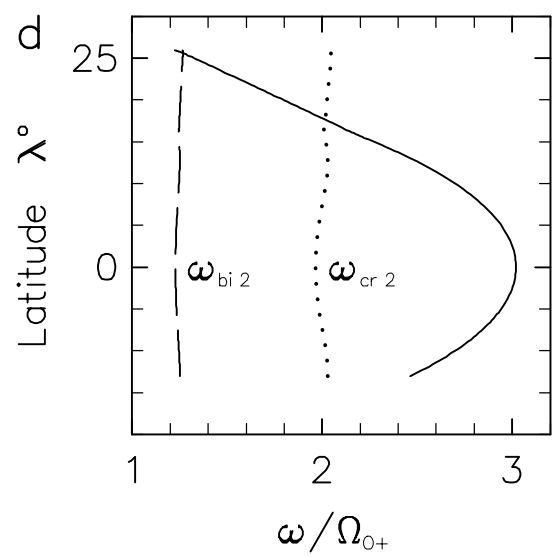
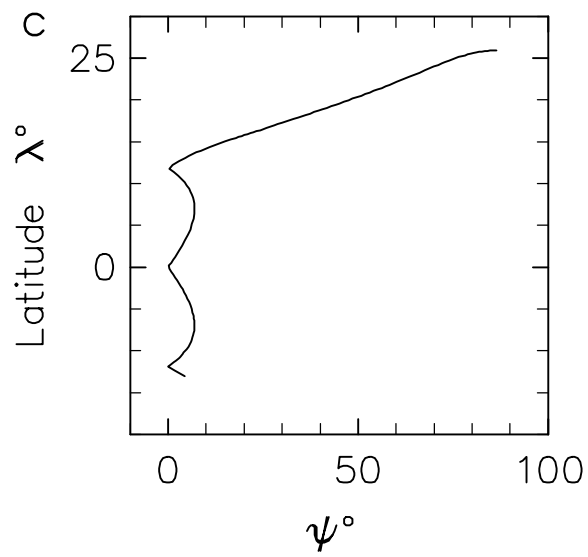
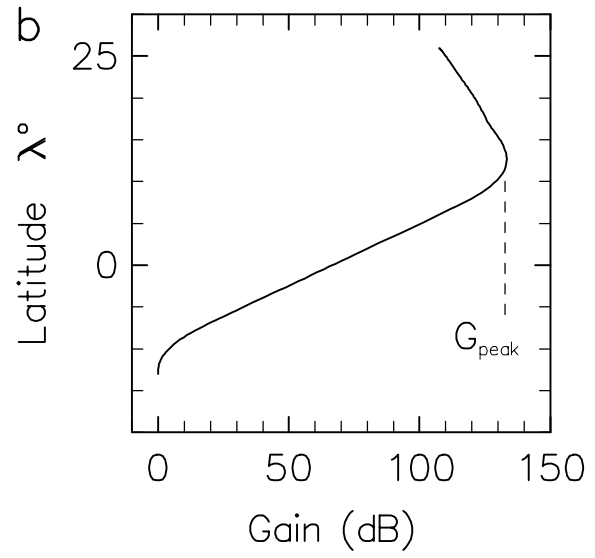
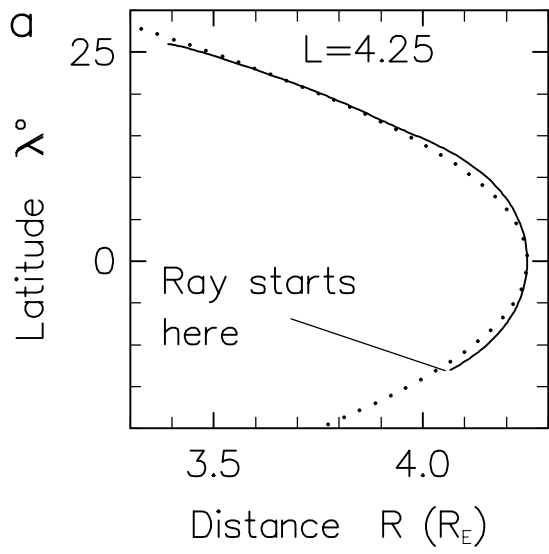
K:\AU_PACKS\GMNEW\TEMPLATE.WPD

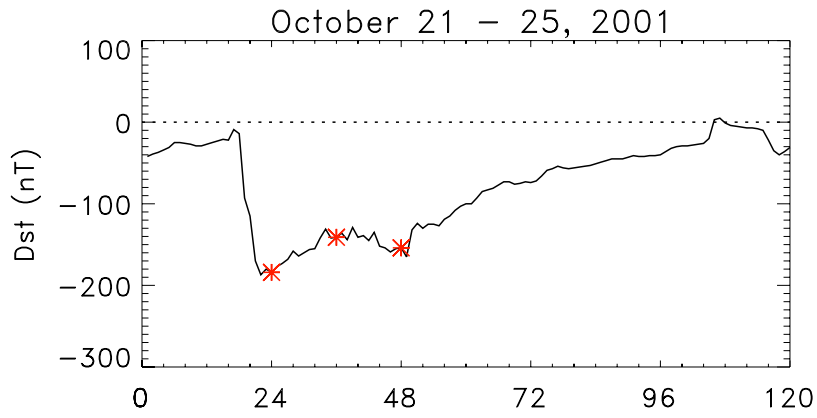


Figure_1_ULF_mono.ps

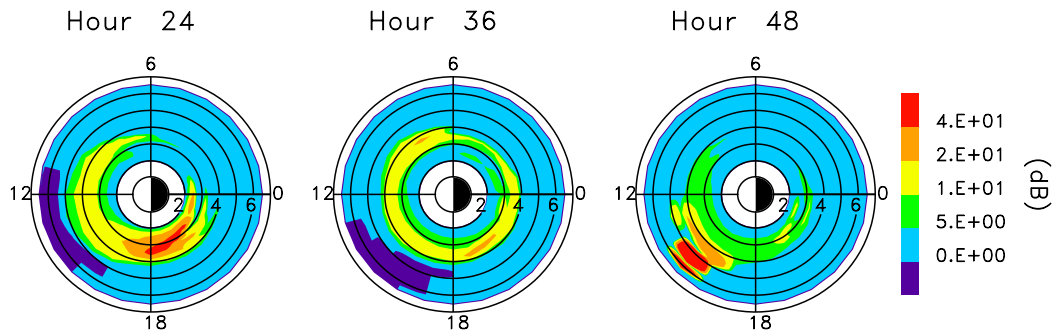


Figure_2_ULF_mono.ps

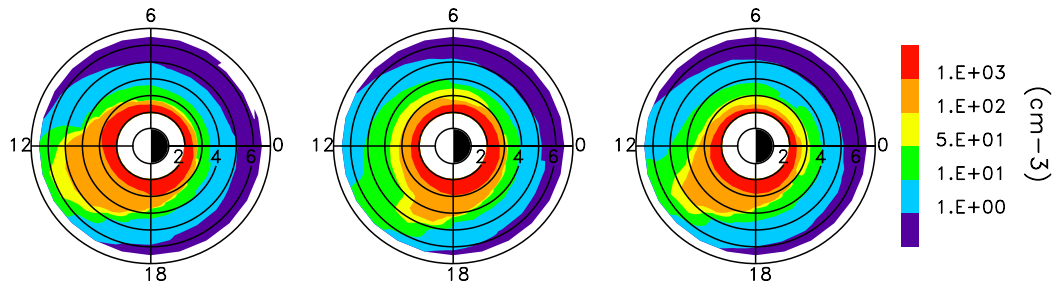




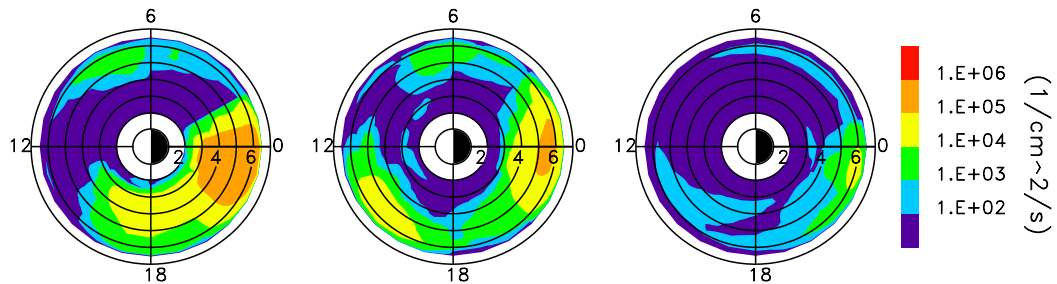
(a) He⁺ Band EMIC Waves



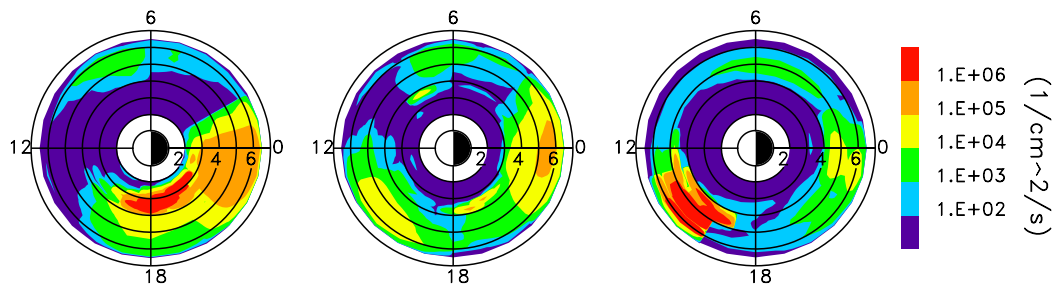
(b) Plasmaspheric Electron Density



(c) Precipitating Proton Flux, No Waves



(d) Precipitating Proton Flux, With Waves



EMIC / H⁺

